

# A Preliminary Comparison of Three Dimensional Particle Tracking and Sizing using Plenoptic Imaging and Digital In-line Holography

Elise D. Munz<sup>1</sup>, Brian S. Thurow<sup>2</sup>  
*Auburn University, Auburn, AL, 36849*

Daniel R. Guildenbecher<sup>3</sup>, Paul S. Farias<sup>4</sup>  
*Sandia National Laboratories, Albuquerque, NM 87185*

**Digital in-line holography and plenoptic photography are two techniques for single-shot, volumetric measurement of 3D particle fields. Here we present a preliminary comparison of the two methods by applying plenoptic imaging to experimental configurations that have been previously investigated with digital in-line holography. These experiments include the tracking of secondary droplets from the impact of a water drop on a thin film of water and tracking of pellets from a shotgun. Both plenoptic imaging and digital in-line holography successfully quantify the 3D nature of these particle fields. This includes measurement of the 3D particle position, individual particle sizes, and three-component velocity vectors. For the initial processing methods presented here, both techniques give out-of-plane positional accuracy of approximately 1-2 particle diameters. For a fixed image sensor, digital holography achieves higher effective in-plane spatial resolutions. However, collimated and coherent illumination makes holography susceptible to image distortion through index of refraction gradients, as demonstrated in the shotgun experiments. On the other hand, plenoptic imaging allows for a simpler experimental configuration. Furthermore, due to the use of diffuse, white-light illumination, plenoptic imaging is less susceptible to image distortion in the shotgun experiments. Additional work is needed to better quantify sources of uncertainty, particularly in the plenoptic experiments, as well as develop data processing methodologies optimized for the plenoptic measurement.**

## I. Introduction

The development of experimental diagnostics for three dimensional (3D) measurements of particle fields is of interest for a wide variety of applications including quantification of 3D fluid flows,<sup>1</sup> investigation of multiphase phenomena,<sup>2,3</sup> and explosion analysis.<sup>4</sup> Historically, two dimensional techniques have been extended to 3D by repeating experiments in multiple planes<sup>5</sup>; however, measurement techniques for instantaneous quantification of a 3D volume are still a developing research area. Two emerging techniques for instantaneous measurement of 3D particle fields are digital in-line holography (DIH) and plenoptic imaging. Here, these two techniques are compared in order to reveal the strengths and weaknesses of each. Before this is done, this paper starts with a brief introduction to each method.

### A. Digital In-line Holography

Digital in-line holography (DIH) is a laser based technique for 3D measurement of a particle field. As illustrated in Fig. 1, DIH is a two-step process comprised of recording and reconstruction. Recording is accomplished by illuminating a particle field with a collimated laser beam and recording the resulting diffraction patterns as a digital hologram. The interference of a conjugate reference wave with the recorded hologram allows for an estimate of the phase and amplitude of the light at the recording plane.<sup>6</sup> By solving the diffraction integral equation, this complex

---

<sup>1</sup> PhD Student, Department of Aerospace Engineering, edm0003@auburn.edu

<sup>2</sup> W. Allen and Martha Reed Associate Professor, Department of Aerospace Engineering

<sup>3</sup> Senior Member of the Technical Staff, Engineering Sciences Center

<sup>4</sup> Laboratory Support Technologist, Engineering Sciences Center

amplitude is numerically refocused to any optical depth,  $z$ , revealing images of particles at their original locations. With appropriately defined processing routines, 3D particle positions and sizes can be automatically measured from recorded holograms.

In Guildenbecher *et al.* 2014<sup>7</sup> DIH was applied to measure the 3D motion of secondary fragments which form from the impact of a water drop on a thin film of water. Figure 1 shows example holograms and the reconstructed 3D particle field. In a second example, Guildenbecher *et al.* 2014<sup>4</sup> applied DIH to study the 3D motion of pellets from a shotgun traveling near sonic conditions (example results are presented in Figure 7). As is discussed in more detail in subsequent sections, these two highly varied experiments illustrate a number of the strengths and weaknesses of the DIH technique. Therefore, by executing these same experiments using plenoptic imaging a reasonable preliminary comparison of the two techniques can be made.

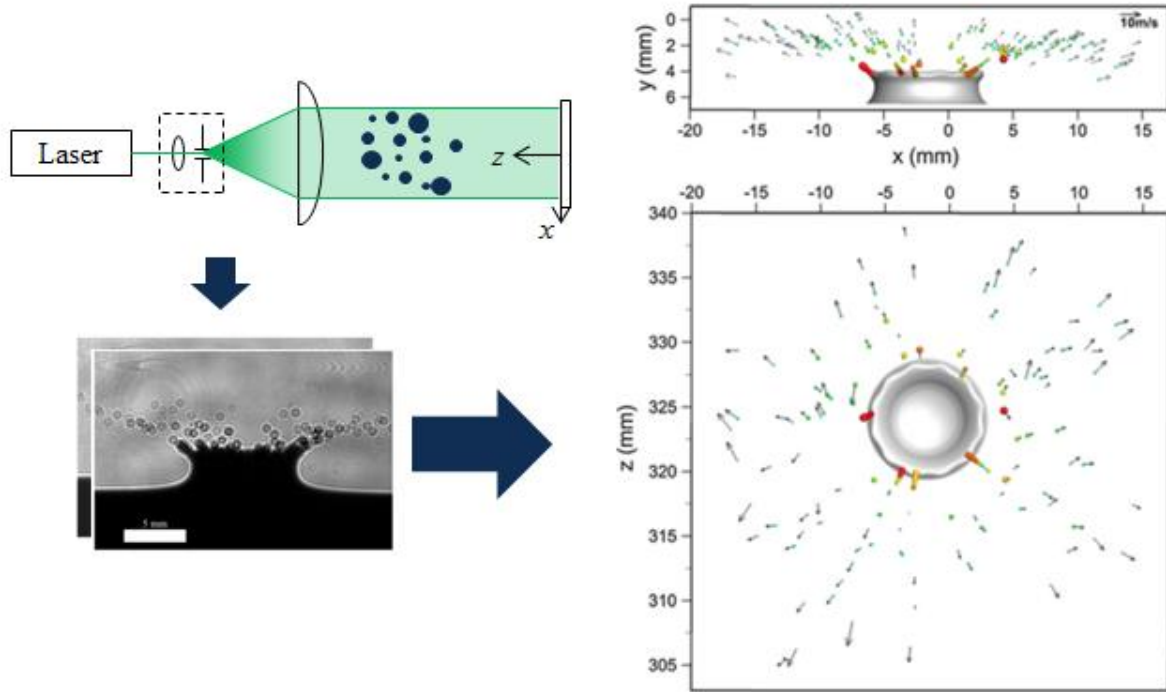


**Figure 1. Digital In-line Holography.** Digital In-line holography (DIH) experimental configuration (top left), example hologram of the splash and secondary fragments when a water drop impacts on a thin film of water (bottom left), and the 3D particle field reconstructed from this hologram (right).<sup>7</sup>

## B. Plenoptic Imaging

Plenoptic imaging is an emerging technology, which allows for instantaneous 3D imaging of a scene using a single camera and white light illumination.<sup>8-10</sup> A conventional camera maps a 3D light field in object space to a 2D image plane such that the angular information of the incoming light is lost. In contrast, a plenoptic camera includes a custom microlens array between the main lens and image sensor. Each microlens creates a sub-image of the light field in the aperture of the main lens, thereby encoding information on the angular distribution of light rays in the aperture plane. With appropriate calibration, each pixel in the sensor plane can be assigned a spatial position based on the center of the microlenses and an angle of propagation based on the location of the pixel within each sub-image. Once discretized in such a manner, the light field is said to be described by a 4D plenoptic function (two spatial coordinates and two angular coordinates). Finally, the plenoptic function can be used to recreate images of the scene at different angular perspectives or numerically refocused along the optical depth.<sup>8</sup> For example, Fig. 2 shows a plenoptic recording of the splash from the impact of a water drop on a thin film of water and images, which have been numerically refocused along the optical depth.

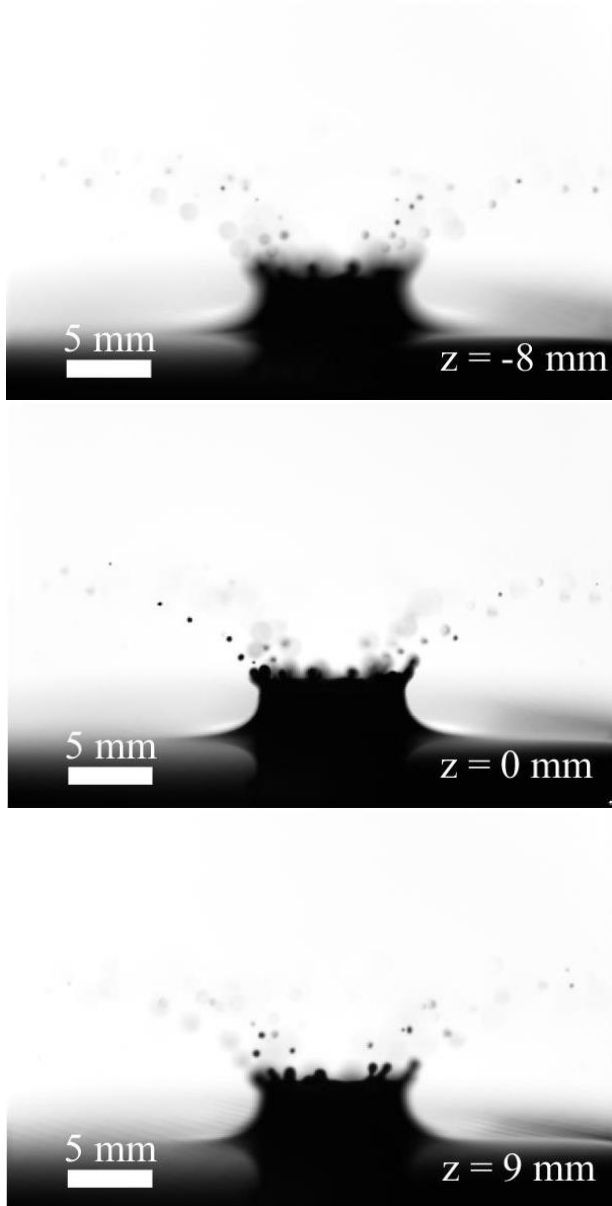


**Figure 2. Refocused Drop Impact Images.** A single raw plenoptic image refocused to three different planes.

As illustrated in Fig. 2, plenoptic cameras capture instantaneous 3D information within a large volume, producing numerically refocused results similar to DIH. Therefore, existing DIH processing algorithms can be modified to extract particle size and location information from refocused plenoptic images.<sup>6</sup> The remainder of this work focuses on application of plenoptic imaging to quantify the secondary fragments, which form from the impact of a water drop on a thin film of water and the 3D motion of pellets from a shotgun traveling at near sonic conditions. With the exception of the use of plenoptic imaging in place of DIH, the experimental configurations replacate our previous investigations of these flows. Consequently, the results provide quantitative comparison of the performance of the two techniques.

Finally, while DIH and plenoptic imaging can produce qualitatively similar results, each method differs significantly in image acquisition and 3D reconstruction. As a result, important quantitative differences are expected between the two techniques. For example, the number of microlenses in the microlens array limits the resolution of the plenoptic refocused images while the resolution of the DIH refocused images is limited only by the resolution of the image sensor. The increased resolution provided by DIH may allow for a more detailed reconstruction of particle size and location, however, the extent of this advantage must be quantified to determine the situations in which it is relevant. On the other hand, plenoptic imaging does not require laser illumination, which DIH necessitates. This not only provides logistical simplification, but may also allow for the use of plenoptic imaging in configurations that permit limited optical access to the volume of interest. Finally, DIH utilizes collimated, coherent light and is susceptible to image distortion through index of refraction gradients,<sup>4</sup> while plenoptic imaging can be performed with diffuse, white light illumination that may be less susceptible to such distortion. For these reasons, a quantitative comparison of the two techniques is warranted in order to determine the experimental applications for which each technique is best suited. This is the focus of the remainder of this work.

## II. Drop Impact Experiment

Here, plenoptic imaging is applied to quantify the motion, size, and shape of secondary fragments produced by the impact of a water drop on a thin film of water.

### A. Experimental Configuration

As was done in Guildenbecher *et al.* 2014<sup>7</sup>, a syringe pump filled with deionized water produced droplets which left a syringe tip at approximately zero velocity and were accelerated by gravity to impact a thin film of deionized water contained in a rubber o-ring affixed to a smooth acrylic surface. The thickness of the film was equal to the height of the o-ring (2.35 mm) and the relatively large diameter of the o-ring (50.8 mm) prevented interaction of the breakup process with the edges. Initial attempts to reconstruct the 3D particle field using our image gradient based techniques were complicated by bright spots caused by light refraction through the transparent drops. This was eliminated by coloring the water with black food dye, resulting in nearly opaque droplets. The surface tension of the

dyed water was measured to be 0.076 N/m, which is equivalent to that of pure deionized water at the same conditions; therefore, it is assumed that the addition of the food dye does not measurably affect the properties of the fluid.

As in the previous DIH experiment, each run was characterized by an impact Weber number,  $We$ , and non-dimensional time,  $\tau$ , calculated using Eqs. (1) and (2), respectively.

$$We = \rho v_0^2 d_0 / \sigma \quad (1)$$

$$\tau = tv_0 / d_0 \quad (2)$$

In these equations and the following discussion,  $\rho$  is the drop density assumed to be 1000 kg/m<sup>3</sup>,  $\sigma$  is the surface tension,  $t$  is the time since impact,  $v_0$  is the impact velocity and  $d_0$  is the initial drop diameter. Due to the slow rate of droplet generation (about 0.06 Hz) it can be assumed that each drop impact occurred on a quiescent surface.

The plenoptic camera used in this work was constructed by the Advanced Flow Diagnostics Laboratory at Auburn University using an Imperx Bobcat B6640 29 MP which has a CoaXPress KAI-29050 CCD image sensor (6600 × 4400 pixels, 5.5 μm pixel pitch) and is modified by the addition of a microlens array with 471 × 362 hexagonally arranged microlenses positioned approximately 308 μm from the image sensor using a custom mount. The pitch of the microlenses is of 77 μm. After plenoptic processing the resolution of the output images is approximately 900 × 600 pixels.

The plenoptic camera was equipped with a 105 mm Nikon macrolens main objective and was positioned to view the impact as shown in Fig. 2. To quantify particle velocities, the interline transfer CCD was operated in double exposure mode and the scene was illuminated with a CaviLux pulsed diode with a wavelength of 640 nm (+/-10 nm) and diffuser. The diode produced two short light pulses approximately 400 ns in duration and 150 μs apart. This resulted in pairs of plenoptic images with an interframe time of 150 μs. Finally, a laser and photodiode were used to produce a trigger signal when the falling droplet interrupted the laser beam. This signal provided a trigger to a Stanford Research delay unit (DG645) which triggered the plenoptic camera after a user specified delay.

With this configuration it was possible to investigate different impact velocities by adjusting the height of the syringe tip and different times since impact by adjusting the Stanford delay unit. The initial analysis presented here considers one fall height (roughly 900 mm) and delay time (4 ms since impact). This condition was chosen to closely match the condition investigated in detail using DIH.<sup>7</sup>

## B. Results and Discussion

Each raw plenoptic image was processed to create a volume made up of a focal stack of 1000 refocused images. These focal stacks were created using the Light Field Imaging Toolkit (LFIT), a collection of MATLAB® functions developed by in the Advanced Flow Diagnostic Laboratory at Auburn University. An example of this focal stack capability is shown in Fig. 2 in which three sample focal planes are displayed from a single instantaneous secondary droplet field. Due to lens distortion it was necessary to dewarp these volumes. The image dewarping function was determined using a 3D second order polynomial fit based on known and measured locations of a dot grid imaged at a variety of depths. After dewarping, the 3D location of each particle was measured from the focal stack using a modified version of the processing algorithm defined in Guildenbecher *et al.* 2013.<sup>6</sup> This algorithm locates particles based on minimum intensity and maximum edge sharpness. Once located in 3D space, individual diameters are measured from the refocused image of each particle. Finally, particle velocities are determined based on a nearest neighbor matching between the 3D particle fields recorded with 150 μs interframe time.

Figure 3 displays two orthogonal views of the measured secondary fragments and their velocities for a sample drop impact case with  $We = 784$  and  $\tau = 5.1$ . This particle field was quantified from the images shown in Fig. 2. The initial drop diameter (3.3 mm) and the impact velocity (4.24 m/s) were calculated from a set of image pairs taken immediately before impact. As expected the secondary droplets generally move radially outward, with uncertainty that appears higher in the out-of-plane,  $z$ , direction compared to the in-plane  $x$ - and  $y$ -directions. In comparing these results to the similar DIH case, both show similar droplet motion and size, however, in the DIH case 196 droplets are identified per realization while in the plenoptic case only 45 droplets are identified per realization. This difference can likely be attributed to the lower spatial resolution of the current plenoptic imaging configuration (40 μm per refocused pixel) compared to the DIH configuration (7.4 μm per pixel). In addition, in this preliminary investigation the plenoptic data has been processed using algorithms adapted from DIH. In the future, it might be possible to define algorithms specifically for plenoptic data which may improve these results, such as the use of deconvolution to remove unwanted blurring.<sup>11</sup>

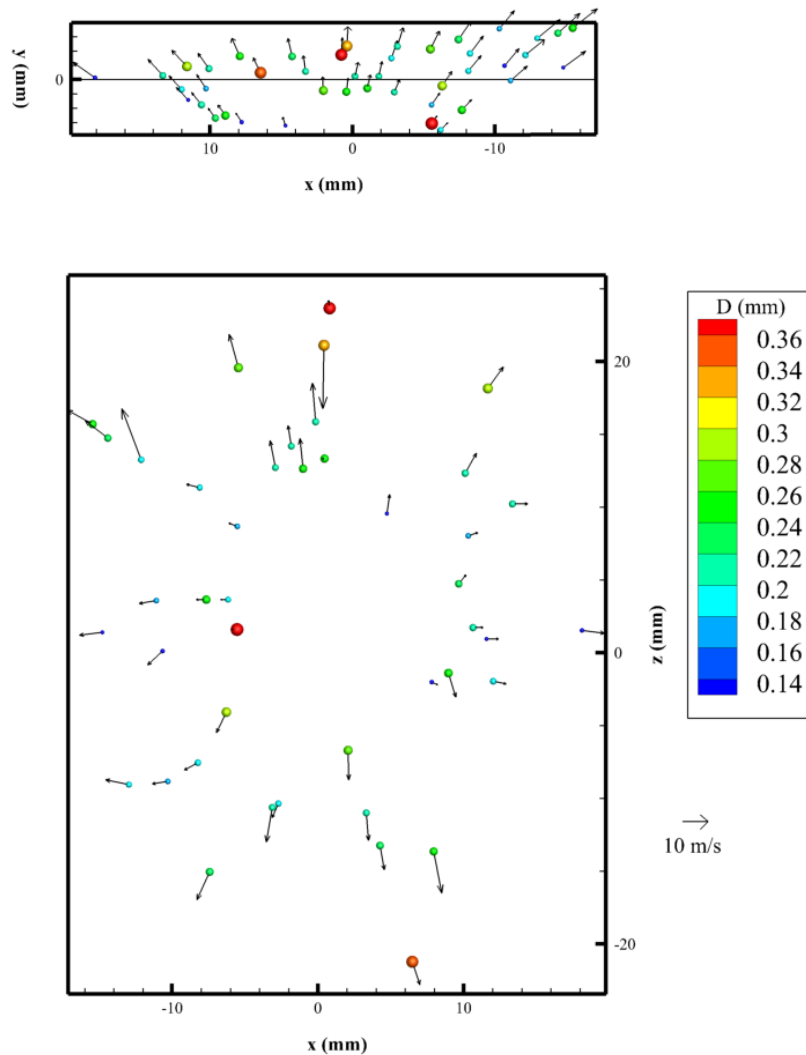


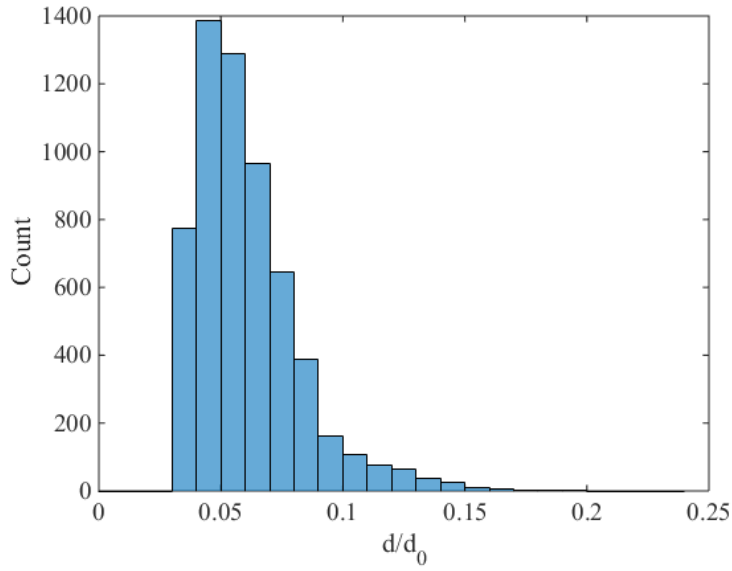
**Figure 3. Measured Three Dimensional Droplet Sizes and Velocities.** Front and top views of the same drop impact, displaying the expected symmetry of the secondary droplet motion in all direction. Several erroneous vectors can also be identified.

uncertainty to positional uncertainty by multiplying by  $v_0 \Delta t$ , the standard deviation of  $z$ -positional uncertainty is approximately 0.75 mean measured particle diameters. For the comparable DIH case, the standard deviation of  $z$ -positional uncertainty was determined to be 0.72 mean measured particle diameters, while over a broader range of experiments the depth uncertainty of DIH was determined to be approximately 1-2 particle diameters.<sup>12</sup> In general, it appears for the conditions and processing methods considered here both DIH and plenoptic imaging give similar depth uncertainties.

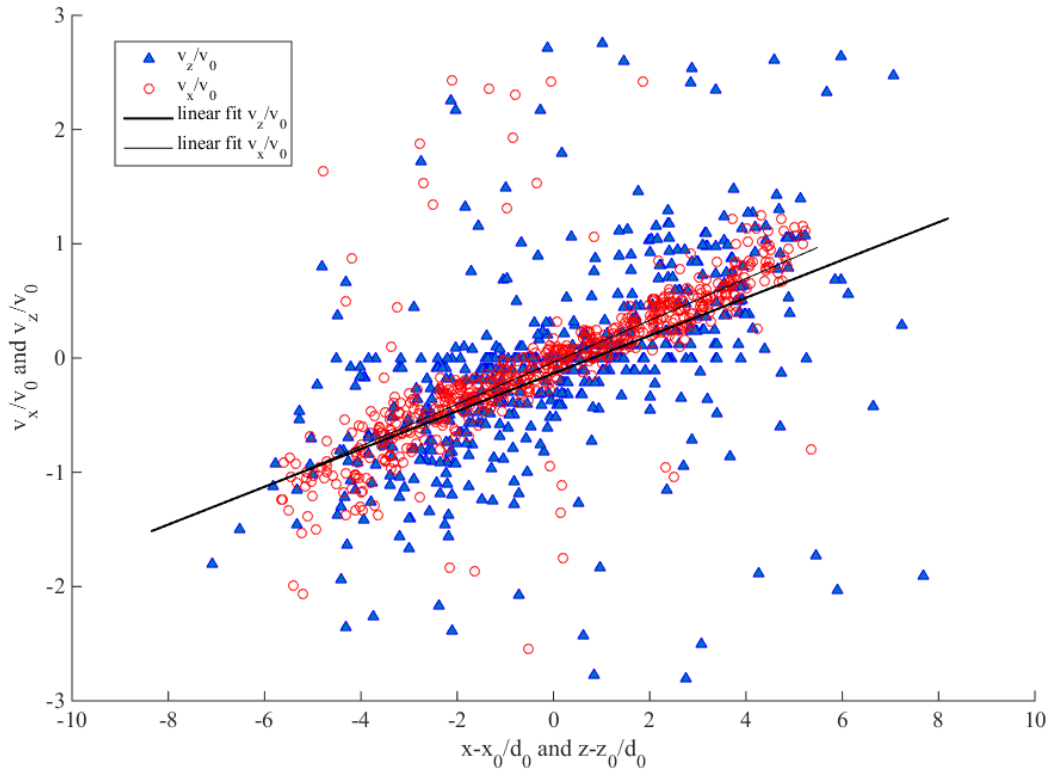
It is interesting to note that when this analysis is redone considering only those drops smaller than the average diameter the standard deviation of  $z$ -positional uncertainty is 0.798 mean measured particle diameters, while when only the drops larger than the average diameter are considered this value is 0.138 mean measured particle diameters. This indicates that the accuracy of the plenoptic imaging system improves for larger particles. This is contrary to the trend in DIH which generally suffers from higher uncertainty as particle size increases.<sup>2</sup> This indicates that plenoptic imaging may be better suited for imaging large particles while DIH is more appropriate for small particles.

Figure 4 shows a histogram of the measured drop size from all realizations at  $We = 784$  and  $\tau = 5.1$ . A notable feature of this data appears in the clipped shape of the lower end of the histogram. This clipping is due to the resolution limit of the plenoptic camera. In this experiment a pixel was approximately 0.01 initial particle diameters, therefore, particles with a diameter approaching this value were not captured using this system.

Figure 5 displays the  $x$ - and  $z$ -velocity components from measured secondary droplets at  $We = 784$  and  $\tau = 5.1$ . Non-dimensional  $x$ -velocity,  $v_x/v_0$ , is plotted as a function of non-dimensional  $x$ -distance from the mean,  $(x-x_0)/d_0$ . The  $z$ -velocities are plotted similarly. Linear fits of  $v_x/v_0$  and  $v_z/v_0$  are also plotted in this figure. The agreement of these two linear fits shows that the mean measured velocities in the  $x$  and  $z$  directions are similar as expected due to flow symmetry. Model error is defined as the difference between the measured velocity component and the velocity component predicted by the linear fit at the measured position. The standard deviation of the model error is calculated to be 0.414 for  $v_x/v_0$  and 0.647 for  $v_z/v_0$ . The difference in these values can be used to approximate the depth uncertainty of the technique by assuming negligible uncertainty in the  $x$ -direction. Converting from velocity



**Figure 4. Measured Drop Size Histogram.** Calculated for all secondary droplets detected at  $We = 784$ ,  $\tau = 5.1$ .



**Figure 5. Measured Non-Dimensional Particle Velocities.** Measured non-dimensional particles velocities  $v_x/v_0$  and  $v_z/v_0$  plotted as a function of non-dimensional distance from the mean  $(x-x_0)/d_0$  and  $(z-z_0)/d_0$ . Linear fits of  $v_x/v_0$  and  $v_z/v_0$  are overlaid on the plot. For clarity, only 10 percent of the calculated points are plotted.

To better understand the main sources of uncertainty in plenoptic imaging, this experiment was repeated at three fall heights and three delay times for a total of nine different conditions. In all cases, the standard deviation in model errors was calculated as above. Our initial analysis indicates that the standard deviation in model errors varies significantly in the  $x$ -direction, while the standard deviation in model errors in the  $z$ -direction is roughly unchanged as a function of experimental conditions. This suggests that the calculated standard deviations in the  $z$ -direction may be constrained by the depth of field of the imaging system and indicates the  $z$ -positional uncertainty may be strongly related to this quantity. More work is needed to fully quantify these observations.

### III. Shotgun Pellet Tracking Experiment

#### A. Experimental Configuration

Again, the experimental configuration was similar to our previous investigation using DIH.<sup>4</sup> A shotgun (12 gauge, number 9 shot) was placed approximately 15 feet from the field of view of the plenoptic camera which was equipped with a 105 mm Nikon macrolens. A breakscreen was used to trigger the camera as the shotgun pellets passed through the screen. The pulsed diode and diffuser provided backlight illumination of the pellets, and two images were recorded for each particle field with an interframe time of  $5\mu\text{s}$ .

#### B. Results and Discussion

Figure 6 shows a plenoptic image pair refocused to two different depths. In these images the pellets propagate right to left. Figure 7 shows a DIH image pair similarly refocused to two different depths. Visual comparison of these figures provides a qualitative comparison of the two imaging methods. The vertical bands in the DIH images are a result of shockwaves visible due to the use of collimated laser light used for illumination. This noise source is not observed in the plenoptic results because they were recorded using diffuse white light. This noise reduction highlights a significant benefit of plenoptic imaging. Another significant difference which can be seen in this figure is the difference in field of view which can be visualized using each method. The field of view used in DIH is limited by the size of collimation lenses, which are difficult and costly to obtain at diameters greater than approximately 50 mm. On the other hand, the field of view of the plenoptic camera can be readily changed by adjusting the focus of the main objective (which, of course, also affects the minimum spatial resolution).

The plenoptic data from this experiment was processed similarly to the drop impact data except that the volumes were not dewarped to correct for aberrations. For the present experiment, this is believed to have a minimal effect on the quantified uncertainties, although more work is needed.

Figure 8 shows a 3D representation of the measured pellet size and motion from one realization. As expected, the particles move primarily in the horizontal,  $x$ , direction, though some uncertainty in the depth,  $z$ , direction is apparent.

The mean particle diameter measured from all realizations is 2.1743 mm with a standard deviation of 0.7836 mm. This is in agreement with expected pellet diameter of approximately 2 mm as defined by the manufacturer specifications. The relatively large standard deviation may arise partly from variations in the actual pellet diameters as well as the incorrect identification of small pieces of the breakscreen as pellets or overlapping pellets as a single particle. Further refinement of the processing algorithms may reduce this standard deviation.

Figure 9 displays a histogram of the displacement in the  $z$  direction calculated using the detected particle matches; the mean displacement is -0.13 mm with a standard deviation of 1.59 mm. This results in an uncertainty, quantified by the standard deviation, of 0.74 mean particle diameters which is again in reasonable agreement with previous estimates of DIH uncertainty of around 1-2 particle diameters.

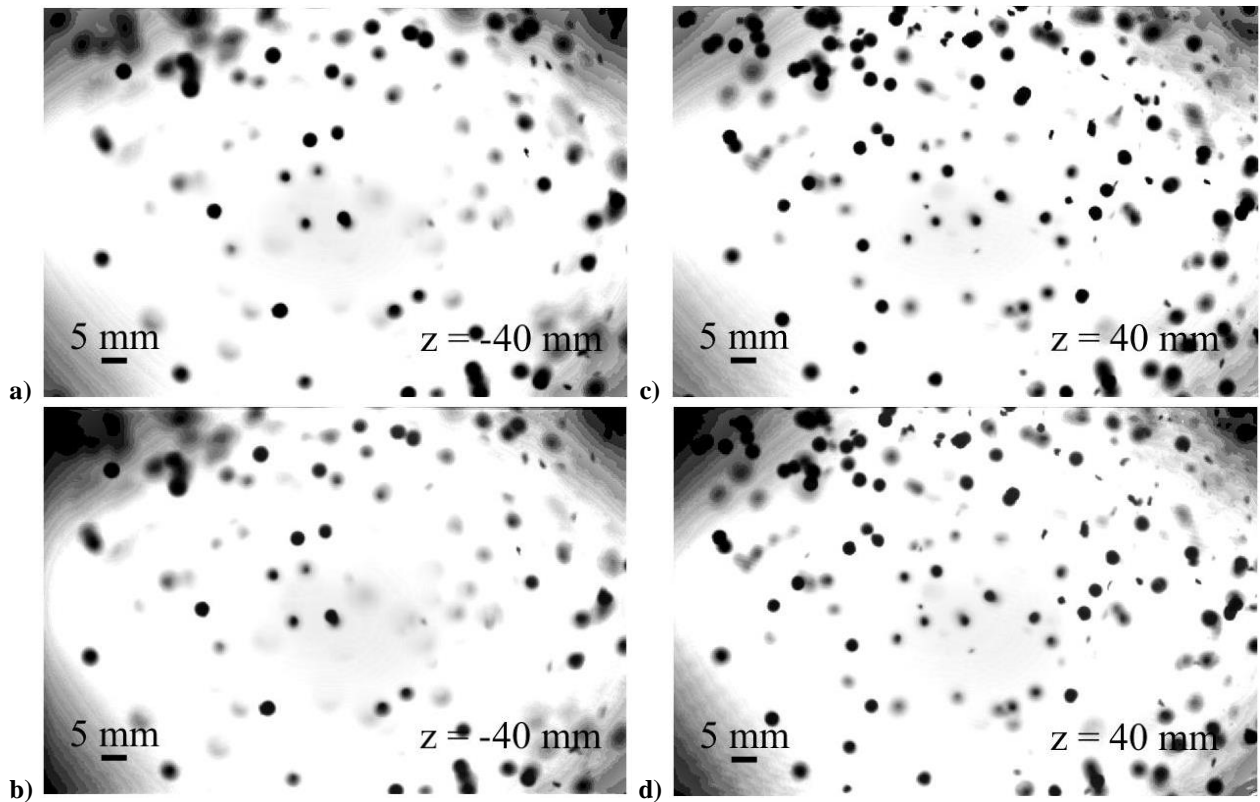


**Figure 6. Refocused Plenoptic Images.** *a,b) Frames 1 and 2 refocused near the front of the volume, c,d) Frames 1 and 2 refocused near the back of the volume.*

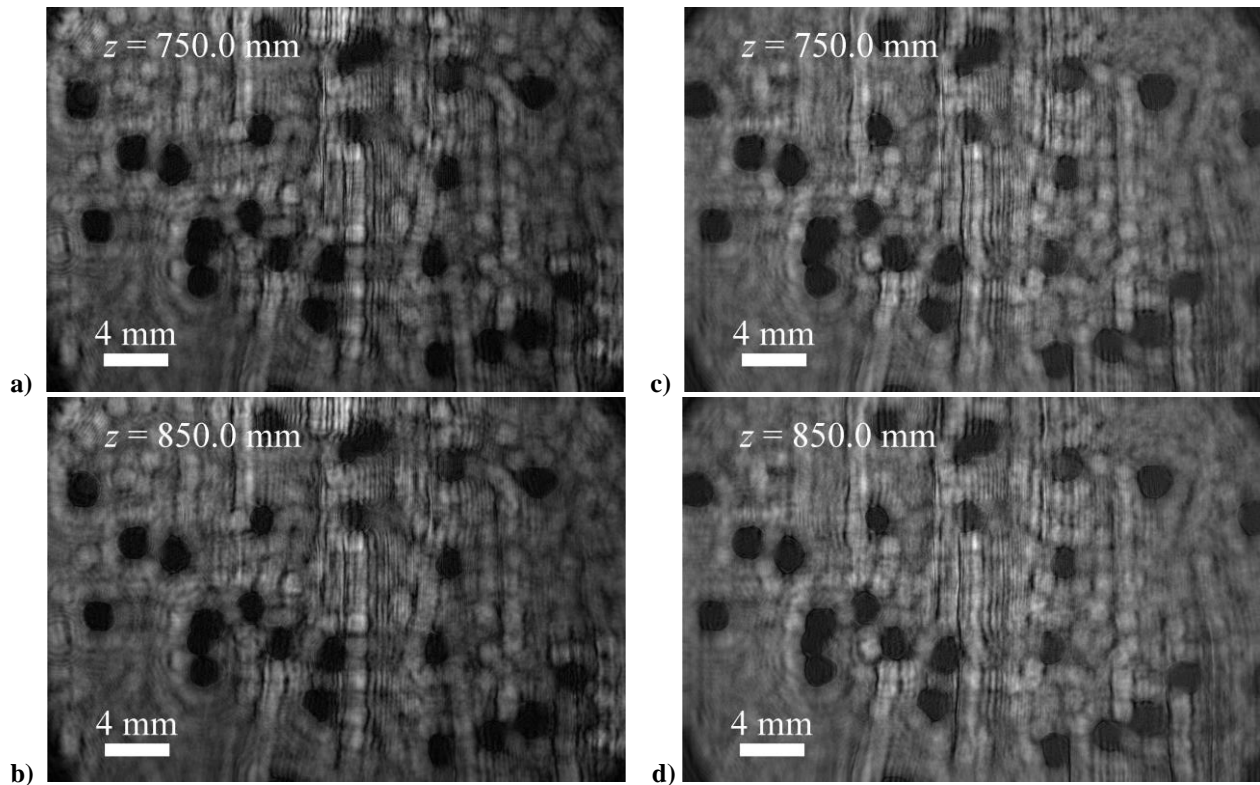


**Figure 7. Refocused DIH Images.** *a,b) Frames 1 and 2 refocused near the front of the volume, c,d) Frames 1 and 2 refocused near the back of the volume.<sup>4</sup>*

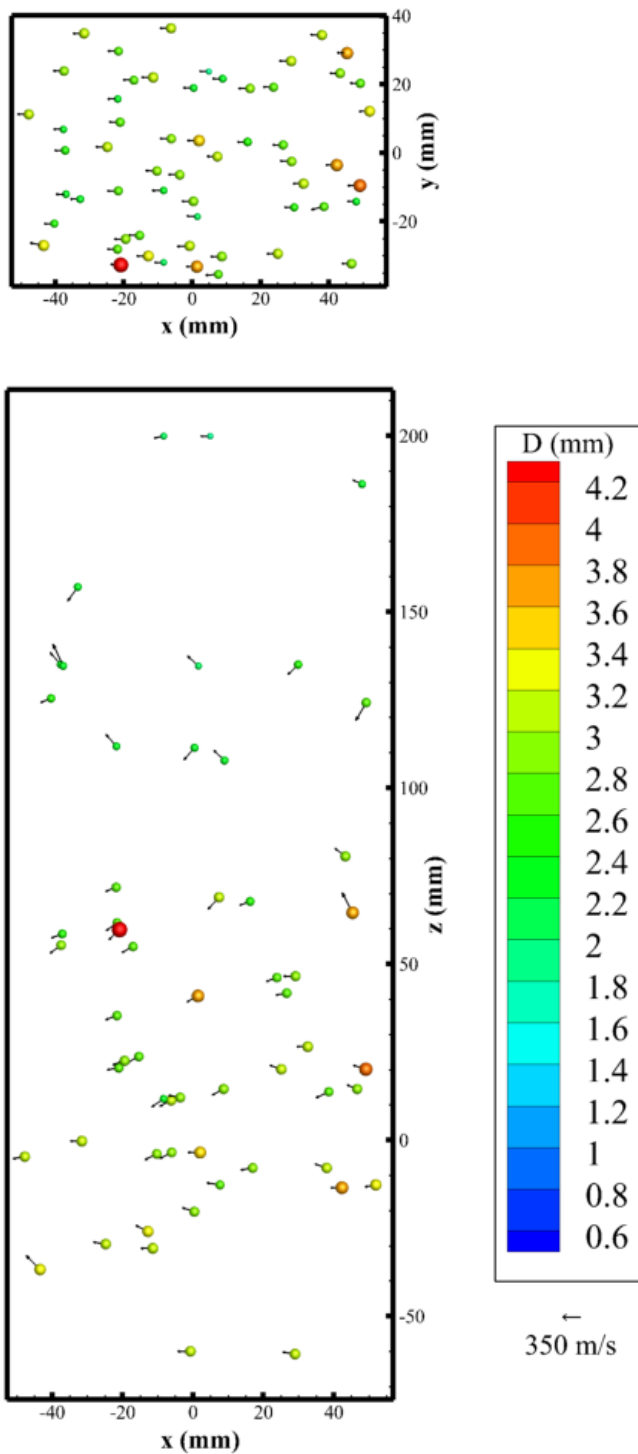


**Figure 8. Shotgun Experiment Vector Plot.** Front and top views of the same shotgun pellet firing. As expected, the detected pellet size shows a small variation and the motion is primarily in the x direction.

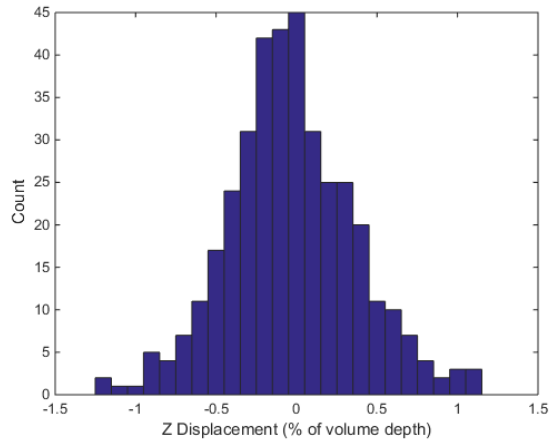


**Figure 9. Z Displacement Histogram.** Histogram displaying Z displacements of particles in all shotgun firings considered. Displacements are shown as a percentage of the total volume depth.

## IV. Conclusion

This work presents a preliminary comparison of diagnostics for measurement of particle size, positions, and velocities in a 3D volume. Digital in-line holography (DIH) is an established technique that reconstructs a 3D volume by numerically refocusing laser diffraction patterns. On the other hand, plenoptic imaging is an emerging technique that utilizes a microlens array to encode angular information of a light field. In this work, plenoptic imaging is applied to quantify the secondary fragments from the impact of a water drop on a thin film of water and the high-speed particles from a shotgun. Results are compared to previous measurements of these flows using DIH. Each technique is shown to have certain advantages and challenges as summarized in Table 1. Other specific conclusions include:

- Both DIH and plenoptic imaging are capable of measuring the 3D nature of the chosen particle fields. This includes an ability to quantify a particle size distribution in a large volume, measure instantaneous 3D position and three-component particle velocities, and reconstruct the expected flow symmetries.
- Both DIH and plenoptic imaging suffer from higher positional uncertainty in the direction normal to the imaging plane. For the configurations and processing algorithms considered here, the out-of-plane positional uncertainty of plenoptic imaging is shown to be around 1 mean particle diameter. This is similar to previous estimates of DIH positional uncertainty of around 1-2 mean particle diameters.
- For a fixed image sensor, DIH tends to have higher spatial resolution compared to plenoptic imaging. As shown in the drop impact results, this limits the dynamic range of particle sizes, which can be quantified in a single experiment.
- By utilizing diffuse light sources, plenoptic imaging is less susceptible to image distortion through index of refraction gradients compared to DIH, which requires collimated and coherent illumination. This is illustrated in the experiments investigating shotgun pellets. The DIH results show clear image distortion due to gas phase shockwaves that exist between the particles, while this effect is not observed in the corresponding plenoptic measurement.

It should also be noted that these experiments do not address all limitations of either technique. In particular, both measurement techniques are challenged when the particle number density increases. More work is needed to determine which, if any, technique is advantageous at high particle densities. In addition, each method currently requires significant computational resources, necessitating the use of a computer cluster to reasonably process the desired volume of data. Although, the algorithms currently implemented have not been optimized for computational efficiency and these requirements are expected to be significantly reduced as improvements are made.

**Table 1. Strengths and weaknesses of each technique.**

	Advantages	Challenges
<b>Plenoptic Imaging</b>	<ul style="list-style-type: none"> <li>• Simple experimental setup requiring limited optical access</li> <li>• Can utilize diffuse, white light illumination sources</li> </ul>	<ul style="list-style-type: none"> <li>• Lower effective spatial resolution</li> <li>• Data processing techniques are not fully developed</li> <li>• Requires custom imaging hardware</li> </ul>
<b>Digital In-line Holography (DIH)</b>	<ul style="list-style-type: none"> <li>• Well established technique, including mature data processing methodology</li> <li>• High spatial resolution</li> <li>• Utilizes commercial hardware, including possibility of high-speed imagers</li> </ul>	<ul style="list-style-type: none"> <li>• Requires collimated laser illumination which increases experimental complexity and can cause unwanted artifacts</li> </ul>

## Acknowledgements

This work has been supported by Sandia National Laboratories, which is a multiprogram laboratory operated by Sandia Corporation, a Lockheed Martin Company, for the United States Department of Energy’s National Nuclear Security Administration under contract No. DE-AC04-94AL85000.

The authors would also like to thank the students of the Auburn University Advanced Flow Diagnostics Laboratory for their work on the development of the Light Field Imaging Toolkit. Finally, we would like to thank Paul Sojka of Purdue University for his assistance with the experimental data acquisition, particularly the surface tension measurements.

## References

- <sup>1</sup> Scarano, F., “Tomographic PIV: principles and practice,” *Measurement Science and Technology*, vol. 24, 2012, p. 012001.
- <sup>2</sup> Katz, J., and Sheng, J., “Applications of Holography in Fluid Mechanics and Particle Dynamics,” *Annual Review of Fluid Mechanics*, vol. 42, 2010, pp. 531–555.
- <sup>3</sup> Gao, J., Guildenbecher, D. R., Reu, P. L., Kulkarni, V., Sojka, P. E., and Chen, J., “Quantitative, three-dimensional diagnostics of multiphase drop fragmentation via digital in-line holography,” *Optics letters*, vol. 38, 2013, pp. 1893–5.
- <sup>4</sup> Guildenbecher, D. R., Reu, P. L., Stuafter, H. L., and Grasser, T., “Accurate measurement of out-of-plane particle displacement from the cross correlation of sequential digital in-line holograms,” *Optics Letters*, vol. 38, 2013, p. 4015.
- <sup>5</sup> Hoyer, K., Holzner, M., Lüthi, B., Guala, M., Liberzon, A., and Kinzelbach, W., “3D scanning particle tracking velocimetry,” *Experiments in Fluids*, vol. 39, 2005, pp. 923–934.
- <sup>6</sup> Guildenbecher, D. R., Gao, J., Reu, P. L., and Chen, J., “Digital holography simulations and experiments to quantify the accuracy of 3D particle location and 2D sizing using a proposed hybrid method,” *Applied Optics*, vol. 52, 2013, pp. 3791–3801.
- <sup>7</sup> Guildenbecher, D. R., Engvall, L., Gao, J., Grasser, T. W., Reu, P. L., and Chen, J., “Digital in-line holography to quantify secondary droplets from the impact of a single drop on a thin film,” *Experiments in Fluids*, vol. 55, 2014.
- <sup>8</sup> Ng, R., Levoy, M., Duval, G., Horowitz, M., and Hanrahan, P., “Light Field Photography with a Hand-held Plenoptic Camera,” *Informational*, 2005, pp. 1–11.
- <sup>9</sup> Fahringer, T. W., Lynch, K. P., and Thurow, B. S., “Volumetric particle image velocimetry with a single plenoptic camera,” *Measurement Science and Technology*, vol. 26, 2015, p. 115201.
- <sup>10</sup> Bichal, A., “Development of 3D Background Oriented Schlieren with a Plenoptic Camera,” Auburn University, 2015.
- <sup>11</sup> Bolan, J. T., “Enhancing Image Resolvability in Obscured Environments Using 3D Deconvolution and a Plenoptic Camera,” Auburn University, 2015.
- <sup>12</sup> Gao, J., Guildenbecher, D. R., Reu, P. L., and Chen, J., “Uncertainty characterization of particle depth measurement using digital in-line holography and the hybrid method,” vol. 21, 2013, pp. 17512–17517.